ELSEVIER

Journal of Atmospheric and Solar-Terrestrial Physics 66 (2004) 1791–1796

Journal of ATMOSPHERIC AND SOLAR-TERRESTRIAL PHYSICS

www.elsevier.com/locate/jastp

Cosmic ray-induced ionization in the atmosphere: spatial and temporal changes

I.G. Usoskin[a,*], O.G. Gladysheva[b], G.A. Kovaltsov[b]

[a]*Sodankylä Geophysical Observatory (Oulu unit), University of Oulu, P.O. Box 3000, 90014 Oulu, Finland*
[b]*Ioffe Physical-Technical Institute, 194021 St.Petersburg, Russia*

Received 5 November 2003; received in revised form 5 May 2004; accepted 4 June 2004
Available online 27 August 2004

Abstract

Detailed calculations of the time-variable spatial distribution of cosmic ray-induced ionization of the lower atmosphere are presented using a physical model. Using the differential energy spectrum of cosmic rays obtained from the worldwide neutron monitor network since 1951 and taking into account also the slow changes in the geomagnetic dipole, we have calculated the corresponding 3D (geographical coordinates and altitude) equilibrium ion concentration in the lower atmosphere as a function of time for the period 1951–2000. A comparison to the results of measurements validates the calculation method, as the calculated cosmic ray-induced ionization reproduces in general the observed altitudinal and latitudinal profiles of the ion concentration. The results of the present work provide a basis for a quantitative study of the solar–terrestrial relationships on long time scales.
© 2004 Elsevier Ltd. All rights reserved.

Keywords: Cosmic ray-induced ionization; Cosmic rays; Atmosphere

1. Introduction

The fields of the atmospheric and space physics overlap in the study of solar-terrestrial relationships. It is a subject of intense debates if there is a strong correlation between low clouds and cosmic ray intensity (e.g., Marsh and Svensmark, 2000; Sun and Bradley, 2002) and what is a physical mechanism responsible for such a relation. One of the most probable candidates for such a mechanism is ionization of the lower atmosphere by cosmic rays which in turn may affect the cloud formation (e.g., Yu, 2002; Marsh and Svensmark, 2003). Most of the earlier studies were concentrating on looking for correlations between clouds and cosmic rays (CR), the latter being represented by a single neutron monitor count rate. Although suitable for correlation study this approach does not allow to build any quantitative (even regression) model. Cosmic rays are the main source of the ionization of lower atmosphere. Primary cosmic rays initiate a nucleonic–electromagnetic cascade in the atmosphere, with the main energy losses at altitudes below 30 km resulting in ionization, dissociation and excitation of molecules (see, e.g., Bazilevskaya and Svirzhevskaya, 1998). Therefore, one needs long data set on spatial distribution and time profiles of the cosmic ray-induced ionization to build quantitative models relating CR to cloud formation. Typical ionization detectors measure not the ambient ion concentration but rather the ion production rate inside themselves. Also, since used as an index of CR, such measurements are performed onboard high-altitude balloon flights at few g/cm^2 of the residual atmosphere (e.g., a review by Bazilevskaya and Svirzhevskaya, 1998). Since there are no routine worldwide measurements of the ion concentrations in the low

*Corresponding author. Fax: +358-8-553-1303.
E-mail address: Ilya.usoskin@oulu.fi (I.G. Usoskin).

1364-6826/$ - see front matter © 2004 Elsevier Ltd. All rights reserved.
doi:10.1016/j.jastp.2004.07.037

atmosphere, we have employed model calculations in this study. In contrast to earlier phenomenological approaches using either parametrization or regression methods (e.g., Heaps, 1978; Hensen and Van Der Hage, 1994; Bazilevskaya et al., 2000), we build a complete physical model which can calculate cosmic ray-induced ionization starting from the solar modulation of CR, without employing any phenomenological regression or parametrization. On the other hand, our model is quite simple in the part calculating the equilibrium ion concentration and does not include complicate ion chemistry.

2. Variations of cosmic ray flux

In order to calculate cosmic ray-induced ionization, one needs to know the flux of cosmic rays impinging on the top of the atmosphere at a given location. This CR flux changes both in time due to the 11-year cycle of the heliospheric modulation and over the Globe due to the geomagnetic shielding. These two processes are discussed below.

Cosmic rays entering the heliosphere suffer from the heliospheric modulation due to the shielding effect of the outward blowing solar wind and the frozen-in interplanetary magnetic field. The modulation results both in reduction of the total CR flux and in hardening of the CR spectrum at 1 AU as the solar cycle progresses from solar minimum to solar maximum (see Fig. 1). The level of modulation changes over the solar cycle together with the heliospheric parameters (solar wind, magnetic field strength and the heliospheric current sheet tilt angle). Unfortunately, more or less regular space-borne direct observations of the galactic cosmic ray (GCR) spectrum are available only during recent years. For earlier times, either fragmentary short-lasting balloon- or space-borne measurement of the CR spectrum or routine observations of ground-based neuron monitors, which are energy-intergrating instruments, are used. We have recently reconstructed the time-variable flux and energy spectrum of cosmic rays for the neutron monitor era since 1951, using the data of the entire world network of neutron monitor from equatorial to polar stations (Usoskin et al., 2002a).

The geomagnetic field results in shielding of GCR entering the Earth's atmosphere so that only CR with rigidity above the so-called geomagnetic rigidity cutoff P_c can penetrate in the atmosphere. The value of P_c depends on the site's location and varies also with time due to slow changes of the geomagnetic field. The significance of the time changes of the geomagnetic field during the last 50 years for the cosmic ray flux impinging on the Earth has been pointed out by Shea and Smart (2003). In order to calculate the local geomagnetic cutoff and its time variations for different locations around the

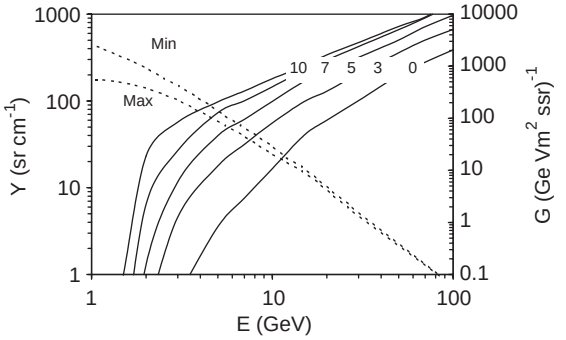

Fig. 1. The ionization yield function Y in polar regions (solid curves, left axis) is shown vs. the energy of primary cosmic rays for different altitudes (in km) as denoted near the curves. The differential energy spectrum of cosmic rays (dotted curves, right axis) is shown for the solar minimum and maximum conditions as denoted next to the curves.

Globe we used an approximation of the shifted geomagnetic dipole. The geomagnetic field is often represented through a series of spherical harmonics (called also Gauss coefficients). Using these spherical harmonics one can calculate the main parameters of the geomagnetic filed such as geographical coordinates of the magnetic poles, position of the dipole center (shifted respect to the Earth's center) and the virtual dipole moment M. Then the local magnetic latitude λ_m of the site can be determined, and finally the local vertical geomagnetic cutoff (in GV) can be estimated using the Størmer's formula (Elsasser et al., 1956)

$$P_c \approx 1.9 M \cos^4(\lambda_m)\left(\frac{R_E}{R}\right)^2, \quad (1)$$

where $R_E = 6371$ km is the mean Earth's radius, R is the distance to the actual dipole center, and M is the virtual geomagnetic dipole moment in 10^{25} G cm^3 ($M = 7.8$ for the 2000 epoch). We used the Gauss coefficients as tabulated in the DGRF/IGRF model (http://nssdc.gsfc.nasa.gov/space/model/magnetos/igrf.html) with 5-year time epochs. Between the epochs we applied a simple linear interpolation of the geomagnetic parameters.

3. Ionization

The ionization of the atmosphere at low and moderate altitudes is fulfilled not by the primary CR particles but by secondaries of a nucleonic–electromagnetic cascade initiated by primary energetic cosmic rays in the Earth's atmosphere. Accordingly, in order to study the cosmic ray-induced ionization, one needs to take into account the development of such a cascade. Here we employed

the CORSIKA Monte Carlo package (Heck et al., 1998) which is specially designed to simulate cascade and includes recent and reliable description of various physical processes and cross-sections. Cosmic rays are assumed to consist of protons and α-particles (≈ 6% in particle number). (When denoting CR energy we mean energy per nucleon, throughout the paper.) In particular, CORSIKA can calculate energy losses deposited by the developing cascade for ionization of the ambient air at every step. First, we have calculated such ionization energy $\Delta E_{\rm ion}(E,X)$ spent by secondaries of the atmospheric cascade initiated by a CR particle with initial energy E, in a thin layer around the residual atmospheric thickness X g/cm^2. The value of $\Delta E_{\rm ion}$ rises with the increasing energy of primary CR particles. The atmospheric layer is assumed to be not too thick (we consider $\Delta X = 25$ g/cm^2 here), i.e., its thickness is small in comparison with the characteristic size of a nucleonic cascade, and atmospheric parameters can be considered roughly constant within the layer. The real width of the layer can be defined as $\Delta h = \Delta X/\rho$, where ρ is the corresponding mean density of the air in this layer. The real altitude h corresponding to the atmospheric thickness X can be calculated as follows:

$$X = a + b\,\exp(-h/c), \tag{2}$$

where coefficients a, b and c are defined from the corresponding atmospheric model. Here we used the standard chemical composition of the atmosphere with the volume fractions of N_2, O_2 and Ar as 78.1%, 21% and 0.9%, respectively (Weast, 1986). As the physical model of the atmosphere we used the well-tabulated US Standard Atmosphere (1976). Assuming that on the average it takes about 35 eV to produce one ion pair in the air (Porter et al., 1976), one can calculate the number of ion pairs produced in one cm layer by the cosmic ray-induced cascade, as follows:

$$q(E,h) = \frac{1}{35\,\mathrm{eV}}\,\frac{\Delta E_{\rm ion}}{\Delta h}. \tag{3}$$

Assuming isotropic flux of primary CR particles and locally flat atmosphere, we can define the "yield function" of cosmic ray-induced ionization, similar to, e.g., yield function of a neutron monitor (e.g., Clem and Dorman, 2000). The concept of the yield function $Y(E,h)$ (Fig. 1) defines the ion-pair production rate corresponding to the mono-energetic unit flux of cosmic rays beyond the Earth's magnetosphere. Then the total ionization rate at a given location can be calculated as the integral of a product of the GCR differential spectrum $G(E)$ and the yield function Y (both are shown in Fig. 1):

$$Q(h) = \int_{P_c}^{\infty} Y(E,h)G(E)\,\mathrm{d}E, \tag{4}$$

where $G(E)$ is the differential energy spectrum of GCR at 1 AU, and P_c is the local geomagnetic rigidity cutoff. The integrand of Eq. (4), i.e. the differential ion production function F, is the product of the sharply decreasing GCR energy spectrum and the increasing yield function, and therefore has a peak-like shape (see Fig. 2). The peak of F-function is broad, with the maximum varying from 1 to 10 GeV depending on the altitudes and phase of the solar cycle. With increasing solar activity this peak moves slightly to higher energies due to the hardening of GCR spectrum, while it moves toward lower energies with increasing altitude. In the neutron monitor terminology it is common to use the effective energy, so that the time profile of GCR flux at this energy is directly proportional to the NM count rate (Alanko et al., 2003), or median energy which halves the integral in Eq. (4) (Ahluwalia and Dorman, 1997). The similarly defined effective/median energy of the cosmic ray-induced ionization at a few km altitude takes the wide range of values from about 10 GeV for polar up to about 50 GeV/nucleon for equatorial sites, which is quite close to the neutron monitors.

We have compared our calculations with the measured ion-pair production rate (Fig. 3), using measurements performed by Neher (1967, 1971) for the solar minimum and by Ermakov et al. (1997) for the solar maximum conditions in both polar and equatorial regions. The agreement between our calculations and the actual measurements is quite good, especially taking into account that the calculations present some average values while measurements were done during short (hours) flights. However, one may notice that predicted values of Q are somewhat lower than measured in the equatorial region. This may be due to a contribution of obliquely incidenting cosmic rays, while our model assumes vertically impinging particles.

Next, we have calculated the equilibrium ion concentration due to cosmic ray ionization, taking into account the recombination processes in the atmosphere.

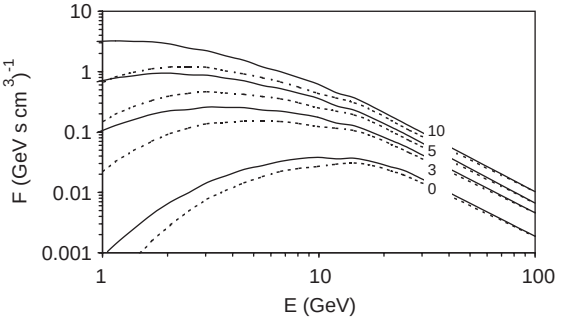

Fig. 2. The differential ion production function F in polar regions vs. the energy of primary GCR corresponding to the solar minimum (solid curves) and solar maximum (dotted curves) conditions for different altitudes as denoted (in km) next to curves.

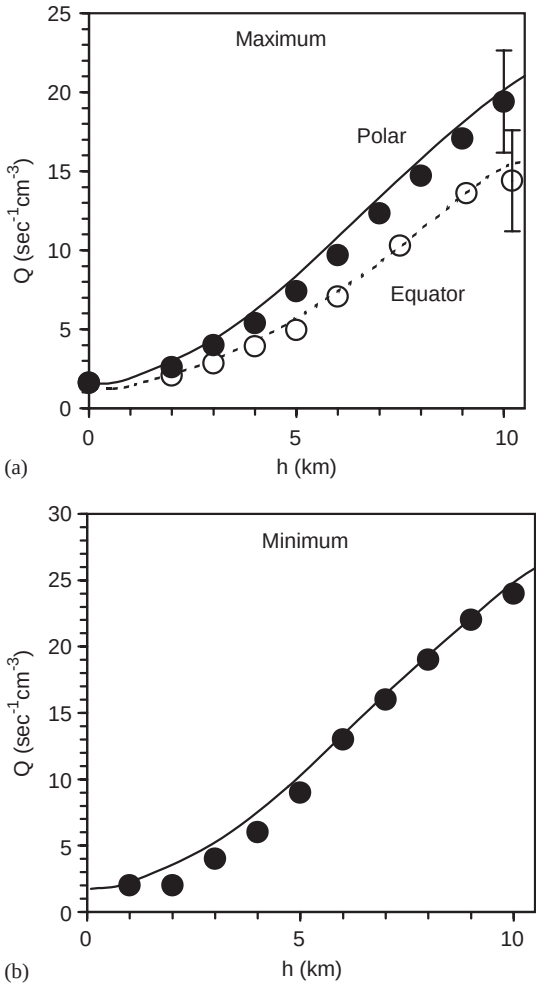

Fig. 3. The altitude profile of the calculated (lines) and measured (dots) ion production rate. Solid/dotted line and filled/open dots denote polar/equatorial regions. (a) Solar maximum, measurements according to Ermakov et al. (1997) with error bars depicting typical errors in defining Q. (b) Solar minimum, measurements according to Neher (1967, 1971).

The equilibrium condition between the ionization rate Q and the ion concentration n is usually considered as follows:

$$Q = \alpha n^2, \tag{5}$$

where α is the recombination coefficient which depends on the local pressure and temperature (e.g., Bates, 1982; Rosen et al., 1982; Smith and Adams, 1982). On the other hand, a possible role of aerosols and "large ions" in the recombination has been discussed (e.g., Ermakov et al., 1997; Bazilevskaya et al., 2000) that may lead to essential deviation from relation (5). In the present study we have adopted the values of the effective recombination coefficient α (Rosen and Hofmann, 1981; Bates, 1982) which agree with the observations. A comparison of the calculated results with the measured ion concentration is difficult since such measurements are indirect and suffer from both local atmospheric parameters fluctuations and systematic uncertainties (e.g., Rosen et al., 1982; Ermakov et al., 1997). Individual measurements undertaken under similar conditions may differ from each other as much as by a factor of 5 (e.g., Chakrabarty et al., 1991; Lehmacher and Offermann, 1997), especially in equatorial regions. In Fig. 4 we have compared the calculated altitude profile of the ion concentration with some measured values of n for both polar and equatorial regions. Polar observations (solid dots) were made by the same instrument during several balloon flights in 1989–1990 (solar maximum). The calculated profile is in a good agreement with the observations for the altitude $\geqslant 7$ km and systematically higher for lower altitudes. However, as mentioned by (Ermakov et al., 1997), this instrument might have missed a fraction of the ions at altitudes below 7 km, resulting in underestimation of the ion concentration. Equatorial observations (open dots) include several short flights performed during 1990's in India (Lehmacher and Offermann, 1997). Although results of individual measurements fluctuate significantly for altitudes below 7 km, the calculation reasonably agrees with the average measured profile.

Thus, using the GCR time-variable flux (Usoskin et al., 2002a), geomagnetic rigidity cut off (Eq. (1)), and the pre-calculated yield function (Fig. 2), we can calculate the ion-pair production rate Q and finally, using Eq. (5), the cosmic ray-induced ionization for a given location and time. Actually we calculate the 3D (longitude, latitude and altitude) time-variable distribution of the cosmic ray-induced ionization. As a snapshot, a surface distribution of the cosmic ray-induced

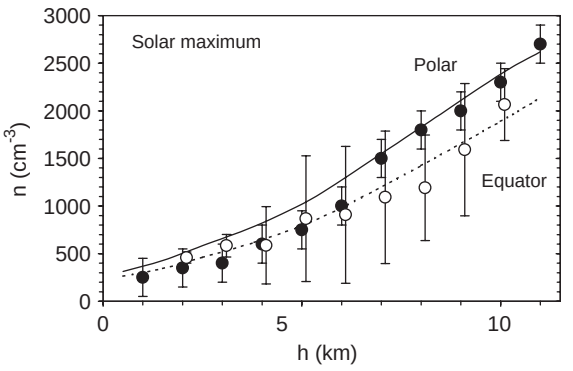

Fig. 4. The altitude profile of the ion concentration for the solar maximum conditions. Solid line and filled dots denote the calculated and the measured (Ermakov et al., 1992, 1997) values of n in polar regions. Dotted line and open dots denote the calculated and the measured (Lehmacher and Offermann, 1997) values of n in the equatorial region ($P_c = 17.3$ GV).

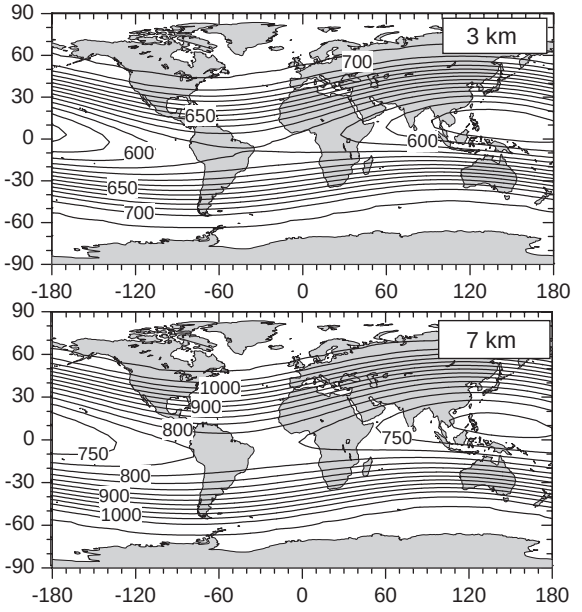

Fig. 5. Calculated cosmic ray-induced ionization for altitudes of about 3 km (upper panel, $X = 725\,g/cm^2$) and about 7 km (lower panel, $X = 425\,g/cm^2$) for the year 2000. Contour lines are given as the number of ion pairs per cm^3 with the step of 10 (25) cm^{-3} in the upper (lower) panel.

ionization is shown in Fig. 5 for the year 2000 for two different altitudes of 3 and 7 km. As expected, the ionization increases with the latitude, changing by 25–40% between the equatorial and polar regions. The ionization is nearly constant beyond the last grid line implying the "knee" in this latitudinal dependence, in agreement with observations (Neher, 1961; Heaps, 1978). This knee at 50–60° geomagnetic latitude corresponds to the geomagnetic cutoff rigidity of 2–2.5 GV. Primary CR particles with lower rigidity/energy do not really contribute to the ion production rate (Fig. 2) at these altitudes, and thus the decreasing effective rigidity cutoff does not result in further increase of the ion concentration here. Next Fig. 6 shows time profiles of the ionization calculated for the 3 km altitude for three different regions: polar, mid-latitudes and equatorial. The amplitude of 11-year cycle variations changes greatly between the polar region (about 80 cm^{-3} or 11% of the solar minimum ionization level) and equatorial regions (about 20 cm^{-3} or less than 5%). The 11-year cycle amplitude in the globally average cosmic ray-induced ionization is about 8%.

4. Concluding remarks

In this paper, we present detailed calculations of the time-variable spatial distribution of cosmic ray-induced ionization of the lower atmosphere. For this purpose, a physical model has been applied including the cosmic ray differential spectrum, Monte-Carlo simulation of the cosmic ray-initiated atmospheric cascade, ion-pair production by the cascade, as well as the balance between ionization and recombination. A comparison of the calculation results with the actual measurements validates the calculation method since no fitting or parametrization has been used in the model. The presented model includes some simplifying assumptions (e.g., vertically impinging cosmic rays, neglect of the real aerosol global distribution), which are subjects to further improvements. However, even with these assumptions the calculated cosmic ray-induced ionization generally reproduces the observed altitudinal and latitudinal profiles of the ion concentration for lower atmosphere (below 10–12 km). The model underestimates the ionization for higher altitudes where the nucleonic cascade is not developed. The present calculations have been carried out for the period since 1951 using the cosmic ray differential flux as computed from the worldwide neutron monitor network data (Usoskin et al., 2002a). However, this calculated series of cosmic ray-induced ionization can be extended backwards in time for about four centuries, using the cosmic ray flux reconstruction since 1610 (Usoskin et al., 2002b).

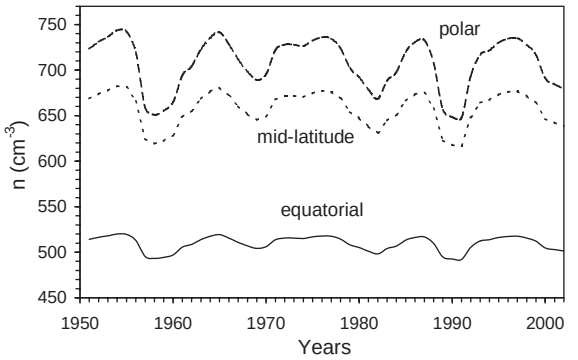

Fig. 6. Calculated time profiles of the annual cosmic ray-induced ionization at the altitude of 3 km ($X = 725\,g/cm^2$, $p = 711$ mb) for three regions: polar ($P_c < 1$ GV), mid-latitudes ($P_c = 6$ GV) and equatorial ($P_c = 15$ GV) regions.

Thus, the results of the present work provide a basis for a quantitative study of the solar–terrestrial relationships on long time scales.

Acknowledgements

We thank Nigel Marsh, Kalevi Mursula and Henrik Svensmark for critical and useful comments. We thank L. Dorman and another referee for useful comments and suggestions on improvements of this paper. The financial support by the Academy of Finland is

acknowledged. GAK has been partly supported by the program "Non-stationary Processes in Astronomy" of Russian Academy of Sciences.

References

Ahluwalia, H.S., Dorman, L.I., 1997. Transverse cosmic ray gradients in the heliosphere and the solar diurnal anisotropy. Journal of Geophysical Research 102, 17433.

Alanko, K., Usoskin, I.G., Mursula, K., Kovaltsov, G.A., 2003. Heliospheric modulation strength: effective neutron monitor energy. Advances in Space Research 32 (4), 615.

Bates, D.R., 1982. Recombination of small ions in the troposphere and lower stratosphere. Planetary Space Science 30 (12), 1275.

Bazilevskaya, G.A., Svirzhevskaya, A.K., 1998. On the stratospheric measurements of cosmic rays. Space Science Review 85, 431.

Bazilevskaya, G.A., Krainev, M.B., Makhmutov, V.S., 2000. Effects of cosmic rays on the Earth's environment. Journal of Atmospheric and Solar-Terrestrial Physics 62, 1577.

Chakrabarty, D.K., Beig, G., Sidhu, J.S., Das, S.R., 1991. Parachute measurements of positive ion density of the middle atmosphere over the dip equator by spherical probe. Journal of Atmosperic and Terrestrial Physics 53, 875.

Clem, J.M., Dorman, L.I., 2000. Neutron monitor response functions. Space Science Review 93, 335.

Elsasser, W., Nay, E.P., Winckler, J.R., 1956. Cosmic-ray intensity and geomagnetism. Nature 178, 1226.

Ermakov, V.I., Kokin, G.A., Komotskov, A.V., Sorokin, M.G., 1992. Results of measurements of the concentration of negative ions in the polar stratosphere. Geomagnetism and Aeronomy 32 (3), 47.

Ermakov, V.I., Bazilevskaya, G.A., Pokrevsky, P.E., Stozhkov, Yu.I., 1997. Ion balance equation in the atmosphere. Journal of Geophysical Research 102 (D19), 23413–23419.

Heaps, M.G., 1978. Parametrization of the cosmic ray ion-pair production rate above 18 km. Planetary Space Science 26, 513.

Heck, D., Knapp, J., Capdevielle, J.N., Schatz, G., Thouw, T., 1998. CORSIKA: A Monte Carlo Code to Simulate Extensive Air Showers, Forschungszentrum Karlsruhe, FZKA 6019.

Hensen, A., Van Der Hage, J.C.H., 1994. Parametrization of cosmic radiation at sea level. Journal of Geophysical Research 99 (D5), 10693.

Lehmacher, G., Offermann, D., (Eds.), 1997. CHRISTA/MAHRSI-Campaign 2 Handbook. Technical Report, University of Wuppertal, D-42097 Wuppertal.

Marsh, N., Svensmark, H., 2000. Low cloud properties influenced by cosmic rays. Physical Review Letters 85, 5004.

Marsh, N., Svensmark, H., 2003. Solar influence on earth's climate. Space Science Review 107, 317.

Neher, H.V., 1961. Cosmic ray knee in 1958. Journal of Geophysical Reseach 66, 4007.

Neher, H.V., 1967. Cosmic ray particles that changed from 1954 to 1965. Journal of Geophysical Reseach 72, 1527–1539.

Neher, H.V., 1971. Cosmic rays at high latitudes and altitudes covering four solar maxima. Journal of Geophysical Reseach 76, 1637–1651.

Porter, H.S., Jackman, C.H., Green, A.E.S., 1976. Efficiencies for production of atomic nitrogen and oxygen by relativistic proton impact in air. Journal of Chemistry and Physics 65, 154.

Rosen, J.M., Hofmann, D.J., 1981. Balloon-borne measurements of electrical conductivity, mobility, and the recombination coefficient. Journal of Geophysical Research 86 (C8), 7406–7410.

Rosen, J.M., et al., 1982. Results of an international workshop on atmospheric electrical measurements. Journal of Geophysical Research 87, 1219.

Shea, M.A., Smart, D.F., 2003. Preliminary study of the 400-year geomagnetic cutoff rigidity changes, cosmic rays and possible climate changes. In: Proceedings of the 28th International Cosmic Ray Conference, Tsukuba, Vol. 7, 4205.

Smith, D., Adams, N.G., 1982. Ionic recombination in the stratosphere. Geophysical Research Letters 9, 1085.

Sun, B., Bradley, R.S., 2002. Solar influences on cosmic rays and cloud formation: a reassessment. Journal of Geophysical Research 107 (D14) AAC 5-1, doi:10.1029/2001JD000560.

U.S. Standard Atmosphere, 1976. U.S. Government Printing Office, Washington, DC.

Usoskin, I.G., Alanko, K., Mursula, K., Kovaltsov, G.A., 2002a. Heliospheric modulation strength during the neutron monitor era. Solar Physics 207, 389.

Usoskin, I.G., Mursula, K., Solanki, S., Schüssler, M., Kovaltsov, G.A., 2002b. Physical reconstruction of cosmic ray intensity since 1610. Journal of Geophysical Research 107 (A11) SSH 13-1, doi: 10.1029/2002JA009343.

Weast, R.C., (Ed.), 1986. Handbook of Chemistry and Physics, sixty-seventh ed., The Chemical Rubber Co., Cleveland.

Yu, F., 2002. Altitude variations of cosmic ray-induced production of aerosols: implications for global cloudiness and climate. Journal of Geophysical Research 107 (A7) SIA 8-1, doi:10.1029/2001JA000248.